Citation &
Copyright (to be inserted by the publisher)

Five-Parameter Grain Boundary Character Distribution in Fe-1%Si

Tricia A. Bennett, Chang-Soo Kim, Gregory S. Rohrer and Anthony D. Rollett

Department of Materials Science and Engineering, Carnegie Mellon University, 5000 Forbes Ave. Pittsburgh, Pennsylvania 15213-3890, USA

Keywords: Iron-silicon steel; Grain boundary character distribution; Grain boundary planes; Grain boundary energy

Abstract. The grain boundary character distribution in an Fe-1%Si steel has been measured as a function of lattice misorientation and boundary plane orientation. There is a weak texture in the space of grain boundary planes that favors the {110} orientation. At specific misorientations, the anisotropy is larger. For example, when the lattice misorientation is 60° around [111], symmetric tilt boundaries comprised of two {110} planes on either side of the interface dominate the population. The results are consistent with observations suggesting that in a range of crystalline materials, the low energy, low index surface planes are found to dominate the distribution of internal interfaces.

Introduction

Five macroscopic parameters are required to distinguish one type of grain boundary from another. In the past, it has been common practice to examine boundary properties as a function of only a subset of these parameters [1,2]. More recently, the distribution and energies of grain boundaries have been measured more comprehensively over all five parameters [3,4]. Following reference [3], we define the grain boundary character distribution, $\lambda(\Delta g, \mathbf{n})$, as the relative areas of grain boundaries characterized by their lattice misorientation (Δg) and orientation ($\mathbf{n}$). Here, similar methods are employed to determine the dependence of the grain boundary population on Δg and $\mathbf{n}$ in a non-oriented electrical steel.

Recent measurements of the grain boundary plane distribution in MgO, $SrTiO_3$, Al, TiO_2, and $MgAl_2O_4$ have revealed an interesting trend [3,5-7]. The most frequently adopted grain boundary planes are the same low index planes that dominate the equilibrium crystal shapes or growth forms of the same materials. In other words, the low energy and slow growing faces observed on the external surfaces of crystals also dominate the distribution of internal surfaces. This implies a correlation surface energy anisotropy, $\gamma(\mathbf{n})$, and the grain boundary energy anisotropy, $\gamma(\Delta g, \mathbf{n})$. This is not too surprising, since both quantities reflect the local disruption in bonding at the interface. The purpose of this work is to determine if the same trend holds in a bcc-structured metal by measuring $\lambda(\Delta g, \mathbf{n})$ for Fe-1%Si.

Methods

Samples. The samples investigated here were from a non-oriented electrical steel alloyed with 1.12 weight percent silicon, referred to hereafter as Fe-1%Si. Minority components in this alloy include (weight %) C: 0.0038, Al: 0.31, Mn:0.61, and N: 0.003. Samples were temper rolled to a reduction in thickness of 8% followed by annealing at 787° C for 1 hour in an $H_2$15% + N_2 85% atmosphere. The final sample thickness was 0.5 mm and the average grain size was 170 μm (0.17 mm). Samples were electropolished to produce a total area of 0.5 cm^2.

Data collection. Crystal orientation maps on the electropolished planar section were obtained using an EBSD mapping system (TexSEM Laboratories, Inc.) integrated with a scanning electron microscope (Phillips XL40 FEG). Each map has an area of 500 μm x 500 μm and the orientations were recorded with a resolution of 20 μm. When all of the smaller maps were combined, there were 17,471 grains in the data set. Cross sectional analysis of the sample showed that the grains were columnar. Therefore, the grain boundaries were orientated perpendicular to the sample plane and each boundary normal was assumed to lie in the section plane perpendicular to the trace of the grain boundary on the section plane. Using a procedure described by Wright and Larsen [8], 5.4×10^4 grain boundary traces were extracted from the orientation maps. Each trace specified the orientation of the two grain boundary planes in the crystals adjacent to the boundary.

The grain boundary character distribution. The procedures for determining the grain boundary character distribution from measurements of the crystal orientations on both sides of the boundary (g_1 and g_2) and the boundary normals in the sample reference frame were described in reference [3]. Briefly, we apply the bicrystal symmetry originally defined by Morawiec [9]. The misorientation must be calculated with respect to both grains:

$$\Delta g = C_{p1} g_1 \left(C_{p2} g_2 \right)^{\mathrm{T}} \text{ and} \tag{1a}$$

$$\Delta g = C_{p2} g_2 \left(C_{p1} g_1 \right)^{\mathrm{T}} \tag{1b}$$

where C_p are the symmetry operators for the cubic system. For cubic crystals, this leads to $2 \bullet 12^2$ equivalent misorientations. For each indistinguishable Δg, we calculate the plane normal in the crystal reference frame (**n**) using the measured planar normal in the sample frame (**n**′) and the non-transposed g_i. In other words, when Δg is calculated using Eq. 1a, $\mathbf{n} = C_{p1} g_1 \mathbf{n}'$, and when Δg is calculated using Eq. 1b, $\mathbf{n} = C_{p2} g_2 \mathbf{n}'$. Finally, we note that it is arbitrary whether the grain boundary normal points into the first or second crystal. This adds an additional factor of two to the number of symmetrically equivalent boundaries so that $2 \bullet 2 \bullet 12^2$ symmetrically equivalent grain boundaries are generated from a single grain boundary trace.

It is convenient to represent $\lambda(\Delta g, \mathbf{n})$ as a finite set of discrete grain boundary types. The three Eulerian angles (ϕ_1, Φ, ϕ_2) used to specify Δg can be parameterized by ϕ_1, $\cos(\Phi)$, and ϕ_2; **n** can be parameterized using the conventional spherical angles θ, and ϕ. The choice of the size of the domain depends on the crystal symmetry. In the complete domain, the five angular parameters, ϕ_1, Φ, ϕ_2, θ, and ϕ range from 0 to 2π, π, 2π, π, and 2π, respectively. For materials with cubic symmetry, it is sufficient to use a sub-domain in which the misorientation parameters range from zero to $\pi/2$, 1, and $\pi/2$ for ϕ_1, $\cos(\Phi)$, and ϕ_2 respectively. This sub-domain is 1/64th of the entire range of possibilities and is a convenient choice because it is the smallest volume that contains an integer number of fundamental zones and can still be partitioned in a simple way. For the cubic system, there are 2304 ($=2 \bullet 2 \bullet 24^2$) general equivalent grain boundaries for every observed segment and 36 (=2304/64) of these are in the sub-domain. Thus each observation is represented by 36 indistinguishable symmetrically equivalent boundaries. Finally, each of the five parameters is partitioned so that each has nine discrete values. This means that the resolution of distribution is approximately 10° and that there are approximately 6,500 different boundary types. Thus, if the boundary normals were randomly distributed, there would be approximately nine observations of each boundary type.

By separating the three misorientation parameters and the two interface plane parameters, the distribution of grain boundary planes at each misorientation, $\lambda(\mathbf{n}|\Delta g)$, can be plotted on a

stereographic projection. Here, the misorientations are selected according to the axis-angle convention by specifying the common axis of rotation, [uvw] and the angle about that axis, ω. The results are presented in multiples of a random distribution (MRD); values greater than one indicate planes observed more frequently than expected in a random distribution.

Results

Based on the EBSD data, the sample exhibited negligible grain orientation. The distribution of grain boundary plane orientations, $\lambda(\mathbf{n})$, averaged over all misorientations, is plotted on the stereographic projection in Fig. 1. The plot shows that the there is very little anisotropy in the distribution of grain boundary planes. Planes with the {110} orientation occur with the highest frequency, but the population is only 10% higher than expected in a random distribution.

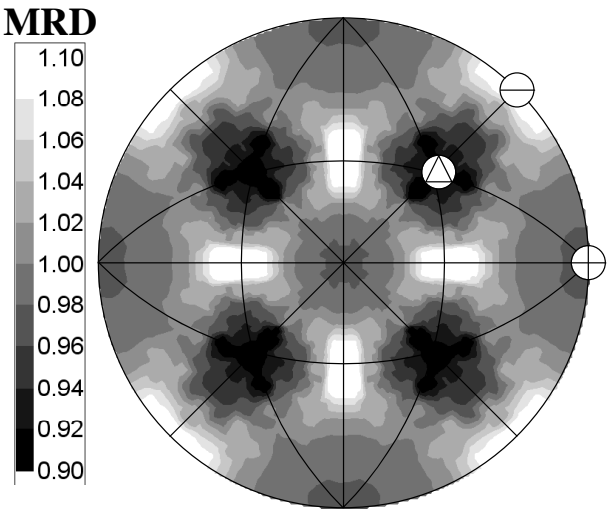

Figure 1. $\lambda(\mathbf{n})$, the relative areas of grain boundary planes in Fe-1%Si, in multiples of a random distribution, plotted in stereographic projection along [001]. The circled triangle, line, and cross denote the [111], [110], and [100] directions, respectively.

At specific locations in the five parameter space, $\lambda(\mathbf{n}|\Delta g)$ is generally larger than in the misorientation averaged plot. At most values of Δg, the boundary plane populations vary from 0.5 MRD to 1.5 MRD. Two examples are shown in Fig. 2, for a 60° rotation about the [110] axis ($\lambda(\mathbf{n}|60°/[110])$) and a 60° rotation about the [111] axis ($\lambda(\mathbf{n}|60°/[111])$). The schematics in 2(a) and 2(b) mark the positions of the misorientation axes, using the same symbols defined in Fig. 1. Grain boundaries that have their surface normal oriented parallel to the misorientation axis are pure twist boundaries. The pure tilt boundaries lie along the great circles that are 90° from the misorientation axes and these positions are marked by the black line in Figs. 2a and 2b. Both of the distributions are consistent with the misorientation averaged finding that {110} type planes are preferred. For example, in Fig. 2c maxima are found at the (110) twist configuration and the $(\bar{1}10)$ tilt configuration. There are also maxima at (101) and $(0\bar{1}1)$, which have mixed tilt and twist components. The only maxima that are not at {110} type positions are those in the zone of the tilt boundaries that are found close to the $(\bar{1}12)$ and $(1\bar{1}2)$ orientations. However, within the angular resolution of the measurement, these planes are the geometrically required complements for the $(\bar{1}10)$ and $(0\bar{1}1)$ asymmetric tilts. In other words, if there is a $(\bar{1}10)$ plane present on one side of

the boundary, then for this misorientation, the plane on the other side of the boundary must be 60° away and in the [110] zone. This point is within 5° of $(\bar{1}12)$.

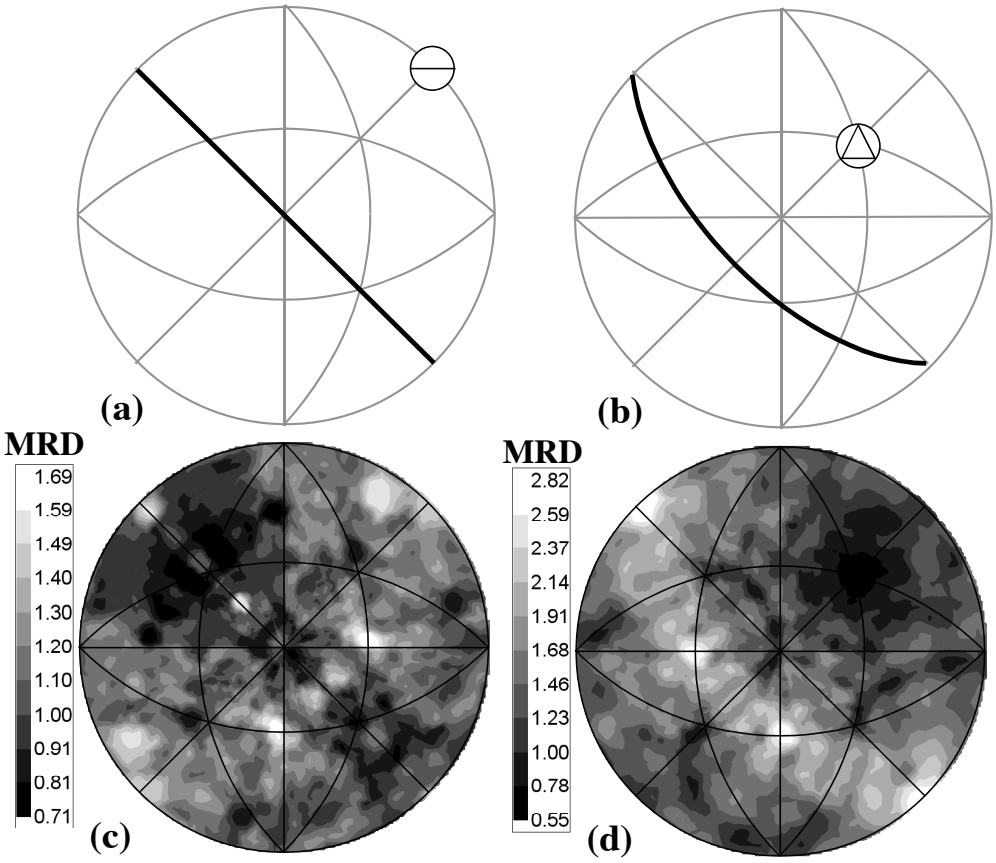

Figure 2. Distribution of grain boundary planes in Fe-1%Si. Schematic illustrations showing the location of twist and tilt boundaries for (a) boundaries with [110] misorientations and (b) boundaries with [111] misorientations. See text for details. (c) $\lambda(\mathbf{n}|60°/[110])$, (d) $\lambda(\mathbf{n}|60°/[111])$. All projections are along [001] and the frame of reference is the same as in Fig. 1.

The distribution in Fig. 2b, $\lambda(\mathbf{n}|60°/[111])$, corresponds to the largest peak in the five parameter distribution. In the coincident site lattice notation, this is also the $\Sigma 3$ boundary. At this point in the misorientation space, it is clear that tilt grain boundaries are strongly favored over all other configurations. The population is greater than one MRD at all positions on the zone of tilt boundaries. Furthermore, the distribution peaks at $(\bar{1}10)$, $(\bar{1}01)$, $(0\bar{1}1)$, and $(1\bar{1}0)$ and this confirms the preference for boundaries terminated on {110} planes. In this case, these planes are exactly 60° apart in the zone of tilts, so both grains on either side of the boundary can be terminated by a {110} type plane.

One other place in the misorientation space that showed significant anisotropy was in the range of low angle boundaries. The distribution of planes for grain boundaries with misorientation angles less than 10° is illustrated in Fig. 3. In this case, the distribution is not sensitive to the axis of misorientation. One artifact of our parameterization of the grain boundary character distribution is that all boundaries with small misorientations (small Euler angles) are grouped in the same discrete cells of the five-dimensional space and because of this, the distribution of planes appears the same for all choices of the misorientation axis. For Fe-1%Si, we see that the population of low angle boundaries is greater than one for all choices of boundary plane and that there are strong peaks at the {210} type positions.

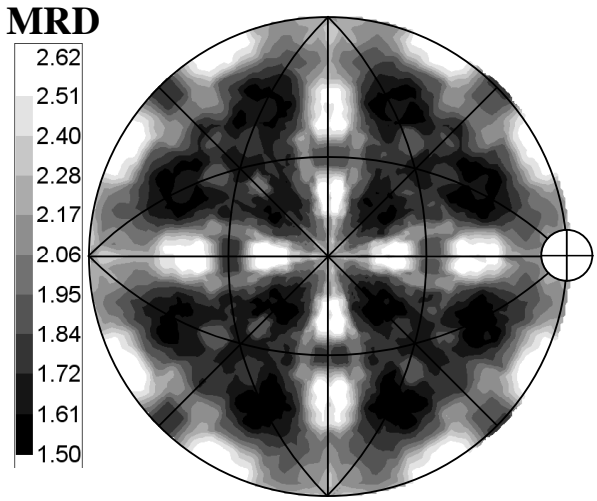

Figure 3. Distribution of planes for low angle grain boundaries. The projection is along [001], in the same reference frame as the other Figures, and the [100] direction is marked by a circle with a cross.

Discussion

As mentioned at the outset, the correlation between the surface energy and grain boundary energy seems reasonable since both reflect the local disruption in bonding at the interface. If we imagine creating a grain boundary by first creating the two free surfaces and then joining them, we can say that the boundary energy is the sum of the two surface energies, minus a binding energy that results from the interactions of the atoms on either side of the interface. Theoretical estimates have shown that the magnitude of the binding energy increases with the average interplanar spacing of the two surfaces adjoining the boundary [10,11]. Since the lowest energy surface planes are those that break the fewest bonds, and these correspond to the densest planes that also have the largest interplanar spacing, we can assume that the surface energies are inversely correlated with the interplanar spacing. So, for a boundary comprised of two low index surfaces, the two surface energies are relatively low and the binding energy is maximized, an effect that leads to a minimum in grain boundary energy for this configuration. Conversely, two high index, high energy surfaces will have a smaller binding energy and represent a maximum in the grain boundary energy.

For the case of Fe-1%Si, the comparison between the grain boundary energy and the distribution of interface planes is not straightforward. In the simplest approximation, we would guess that since the (110) surface has the largest interplanar spacing and can be created by breaking the fewest bonds, it should have the lowest surface energy. This is consistent with our observations. On the other hand, detailed measurements of the surface energy anisotropy of Fe-3%Si show that while this the case at some temperatures, there are conditions where the (100) surface has a lower energy (at temperatures greater than 1300°C) and where the (111) surface has a lower energy (a low temperature where oxygen is adsorbed on the surface) [12,13]. The fact that these low index surfaces have comparable energies may be the reason that the anisotropy of the five parameter grain boundary distribution is smaller than has been observed in other materials. Throughout the majority of the space, the population of grain boundary planes varies from 0.5 to 1.5 MRD. The peak near three MRD for the symmetric {110} tilt boundary is the largest in the five parameter space. The anisotropies in the population in other materials were much larger. For the ceramics materials, such as MgO, $SrTiO_3$, $MgAl_2O_4$, and TiO_2, this is expected since the anisotropy of the surface energy is

relatively large [6]. On the other hand, the surface energy anisotropy of commercially pure Al is not expected to be significantly more than Fe-1%Si, yet the anisotropy in the distribution of grain boundary planes was observed to be larger [6]. In any case, the fact that the most common boundaries plane corresponds the to densest plane with the fewest broken bonds is consistent with the earlier observations [3, 5-7].

The distribution of grain boundary planes for low angle boundaries is difficult to understand. Such boundaries are formed by arrays of dislocations. Boundaries that create a misorientation with the minimum number of dislocations are preferred and these are typically boundaries that are perpendicular to the Burgers vector of the dominant dislocation. For bcc metals, the most common dislocations have <111> Burgers vectors, but these are not perpendicular to the {210} planes.

Summary

The distribution of grain boundary planes in Fe-1%Si is weakly anisotropic, showing a preference for internal grain surfaces with the {110} orientation. The results are consistent with observations suggesting that in a range of crystalline materials, dense, low index surface planes, which typically have low energies and low growth rates, dominate the distribution of internal interfaces.

Acknowledgment

This work was supported by the MRSEC Program of the National Science Foundation under award number DMR-0079996.

References

[1] C.G. Dunn and F.J. Lionetti: Trans. AIME Vol. 185 (1949), p. 125.

[2] Yu.S. Avraamov, A.G. Gvozdev, V.I. Glushkov, and B.G. Livshits: Fiz. Metal. Metalloved., Vol. 25 (1968), p. 831.

[3] D.M. Saylor, A. Morawiec, and G.S. Rohrer: Acta Mater. Vol. 51 (2003), p. 3663.

[4] D.M. Saylor, A. Morawiec, and G.S. Rohrer: Acta Mater. Vol. 51 (2003), p. 3675.

[5] D.M. Saylor, B.S. El-Dasher, T. Sano, and G.S. Rohrer: J. Amer. Ceram. Soc. In press.

[6] D.M. Saylor, B.S. El Dasher, Y. Pang, H.M. Miller, P. Wynblatt, A.D. Rollett, and G.S. Rohrer: J. Amer. Ceram. Soc. In press.

[7] H.M. Miller, D.M. Saylor, B.S. El Dasher, A.D. Rollett, and G.S. Rohrer: this volume.

[8] S.I. Wright and R.J. Larsen: J. Micro. Vol. 205 (2002) p. 245.

[9] A. Morawiec, in: H. Weiland, B.L. Adams, A.D. Rollett (Eds.) Proceedings of the Third International Conference on Grain Growth (TMS, Warrendale, PA, 1998), p. 509.

[10] A.P. Sutton: Prog. Mater. Sci. Vol. 36 (1992) p. 167.

[11] D Wolf and S. Phillpot: Mater. Sci. and Eng. Vol. A 107 (1989), p. 3.

[12] B. Gale, R.A. Hunt and M. McLean: Phil. Mag., Vol. 25 (1972), p. 947.

[13] B. Mills, M. McLean, and E.D. Hondros: Phil. Mag., Vol. 27 (1973), p. 361.